



## Fourier transform emission spectroscopy of the $E^2\Pi-X^2\Sigma^+$ transition of BaH

R.S. Ram<sup>a,\*</sup>, P.F. Bernath<sup>a,b</sup>

<sup>a</sup> Department of Chemistry, University of York, Heslington, York YO10 5DD, UK

<sup>b</sup> Department of Chemistry and Biochemistry, Old Dominion University, Norfolk, VA 23529, USA

### ARTICLE INFO

#### Article history:

Received 26 October 2012

In revised form 11 December 2012

Available online 26 December 2012

#### Keywords:

Electronic spectra  
Alkaline earth hydrides  
Rotational analysis  
Equilibrium constants

### ABSTRACT

The emission spectra of  $E^2\Pi-X^2\Sigma^+$  transition of BaH have been reinvestigated at high resolution using the Fourier transform spectrometer associated with the McMath–Pierce Solar Telescope of the National Solar Observatory. Bands observed in the  $\Delta v = 0$  sequence have been measured and a rotational analysis of the 0–0, 1–1 and 2–2 bands has been obtained. The present measurements have been combined with the previous infrared vibration–rotation measurements of the ground state to provide improved spectroscopic constants for the  $E^2\Pi$  state. The principal spectroscopic constants of this state obtained from this analysis are:  $\omega_e = 1221.912(12) \text{ cm}^{-1}$ ,  $\omega_e x_e = 15.6682(60) \text{ cm}^{-1}$ ,  $B_e = 3.520609(41) \text{ cm}^{-1}$  and  $r_e = 2.187651(13) \text{ \AA}$ .

© 2013 Elsevier Inc. All rights reserved.

### 1. Introduction

The emission spectra of BaH are known since 1932 when Fredrickson and Watson [1] observed a  $^2\Pi-^2\Sigma^+$  transition in the  $14400\text{--}15600 \text{ cm}^{-1}$  region using a metallic barium arc in a hydrogen atmosphere. This transition was subsequently studied by Funke [2] who obtained a rotational analysis of several bands. This study was followed by the observation of several near infrared bands by Watson [3] and Koontz and Watson [4]. These bands were classified into two new transitions:  $^2\Pi-^2\Sigma^+$  and  $^2\Sigma^+-^2\Sigma^+$ . These three transitions were later labeled as A–X, B–X and E–X in order of increasing energy. Transitions involving many higher-lying electronic states  $D^2\Sigma^+$  [5],  $C^2\Sigma^+$  [6,7],  $F^2\Sigma^+$  [8,9],  $G^2\Sigma^+$  [9],  $I^2\Sigma^+$  [10],  $K^2\Sigma^+$  [11],  $L^2\Pi$  [11] and  $M^2\Sigma^+$  [12] have also been observed.

The  $A^2\Pi-X^2\Sigma^+$  [13] and  $B^2\Sigma^+-X^2\Sigma^+$  [14] transitions of BaH have been studied extensively at high resolution. The analysis of the  $A^2\Pi-X^2\Sigma^+$  transition by Kopp et al. [13] provided evidence for the presence of an unobserved low-lying  $H^2\Delta$  state from the observed perturbations in the  $A^2\Pi-X^2\Sigma^+$  bands. This  $H^2\Delta$  state was later directly observed by Fabre et al. [15] in a laser-induced fluorescence study, in which the  $E^2\Pi-X^2\Sigma^+$  bands in the visible region were excited using a tunable laser and fluorescence in the visible and the near infrared regions was monitored with a Fourier transform spectrometer. The observed fluorescence was found to correspond to the  $E^2\Pi-X^2\Sigma^+$ ,  $E^2\Pi_{3/2}-A^2\Pi_{3/2}$ ,  $E^2\Pi-B^2\Sigma^+$  and  $E^2\Pi_{3/2}-H^2\Delta_{5/2}$  transitions. The  $A^2\Pi$ ,  $B^2\Sigma^+$  and  $H^2\Delta$  states form a group of interacting states which correlate with the  $Ba, \dots, 6s5d^3D$  atomic

state. The perturbations in the  $H^2\Delta-A^2\Pi-B^2\Sigma^+$  complex have been extensively examined experimentally [16–18]. Barrow et al. [18] have studied the intensities of the forbidden  $H^2\Delta-X^2\Sigma^+$  transition of BaH, and concluded that some branches become allowed due to mixing of the  $H^2\Delta$  state with the nearby  $A^2\Pi$  and  $B^2\Sigma^+$  states. There are several theoretical studies of the electronic structure of BaH [19–22]. In a recent study, Allouche et al. [22] have predicted the spectroscopic properties of a large number of electronic states of BaH. They have also studied the interaction between the  $H^2\Delta-A^2\Pi-B^2\Sigma^+$  states theoretically.

Radiative lifetime measurements have been obtained for the  $B^2\Sigma^+$  state by Berg et al. [23] using the laser resonance method. It was found that the lifetime varies with rotational quantum number because of interaction between  $A^2\Pi$ ,  $B^2\Sigma^+$  and  $H^2\Delta$  states. A lifetime of  $125 \pm 2 \text{ ns}$  was obtained for the  $v=0$  vibrational level at  $J=5.5$  of the of the  $B^2\Sigma^+$  state. Knight and Weltner [24] have studied the ground state hyperfine interaction and chemical bonding for BaH.

The vibration–rotation transitions in the  $X^2\Sigma^+$  ground electronic state have been measured by Magg et al. [25] and more recently by Walker et al. [26]. Magg et al. [25] have measured vibration–rotation transitions of the four isotopic forms of barium monohydride,  $^{138}\text{BaH}$ ,  $^{137}\text{BaH}$ ,  $^{136}\text{BaH}$  and  $^{135}\text{BaH}$  in the  $1 \leftarrow 0$ ,  $2 \leftarrow 1$  and  $3 \leftarrow 2$  bands by diode laser spectroscopy, while Walker et al. [26] have obtained more extensive measurements in the same bands using Fourier transform emission spectroscopy.

In the present paper we report on the high resolution study of the  $E^2\Pi-X^2\Sigma^+$  transition of BaH. Although data are available for the low-lying electronic states  $A^2\Pi$  [5] and  $B^2\Sigma^+$  [6] from studies of the  $A^2\Pi-X^2\Sigma^+$  and  $B^2\Sigma^+-X^2\Sigma^+$  transitions, no modern high resolution data are available for the  $E^2\Pi$  state (except for the 0–0 band

\* Corresponding author. Fax: +44 0 1904 432516.

E-mail address: rr662@york.ac.uk (R.S. Ram).

by Fabre et al. [15]) since the observation of this state in the early 1930s. We have also included the available infrared data [25,26] with our measurements in order to obtain improved spectroscopic constants for the  $E^2\Pi$  state.

## 2. Experiment

The spectra were recorded on 11/17/1983 using the 1-m Fourier transform spectrometer associated with the McMath–Pierce Solar Telescope of the National Solar Observatory. The spectra of BaH were produced in a barium hollow cathode lamp operated with Ar gas. The lamp was operated at 150 V with 300 mA current and a slow flow of 0.7 Torr Ar and  $\sim 40$  m Torr of  $H_2$ . The spectra of BaH in the  $13500\text{--}15900\text{ cm}^{-1}$  range were recorded using the UV beamsplitter, midrange diode detectors and a zero dispersion monochromator acting as a filter. A total of four scans were co-added in about 30 min of integration at  $0.015\text{ cm}^{-1}$  resolution. The maximum signal-to-noise ratio of 76:1 was determined for the strong and unblended rotational lines.

The spectral line positions were extracted from the observed spectra using a data reduction program called PC-DECOMP developed by J. Brault. The peak positions were determined by fitting a Voigt line shape function to each spectral feature. In addition to the BaH bands, the spectra also contained many Ba and Ar atomic lines and the BaH lines were calibrated using the Ar line measurements by Whaling et al. [27]. The absolute accuracy of the wave number scale is expected to be better than  $\pm 0.003\text{ cm}^{-1}$ . However, uncertainty in the measurement of weaker lines is expected to be somewhat higher depending on the extent of blending, line broadening, and the signal-to-noise ratio.

## 3. Results and discussion

The  $E^2\Pi\text{--}X^2\Sigma^+$  transition of BaH consisting of the  $\Delta v = 0$  sequence is located in the  $14000\text{--}15500\text{ cm}^{-1}$  region. The bands of this transition are highly diagonal and intensity of higher vibrational bands falls rapidly with increasing  $v$  values. The bands belonging to the  $\Delta v \neq 0$  sequences were not recorded in our spectrum. We have measured and analyzed the spectra of the 0–0, 1–1 and 2–2 bands. The 3–3 band is also present very weakly, but it could not be rotationally analyzed because of limited data. A compressed portion of this spectrum is presented in Fig. 1, in which the  $^2\Pi_{1/2}\text{--}^2\Sigma^+$  and  $^2\Pi_{3/2}\text{--}^2\Sigma^+$  sub-bands of the 0–0 band have been marked.

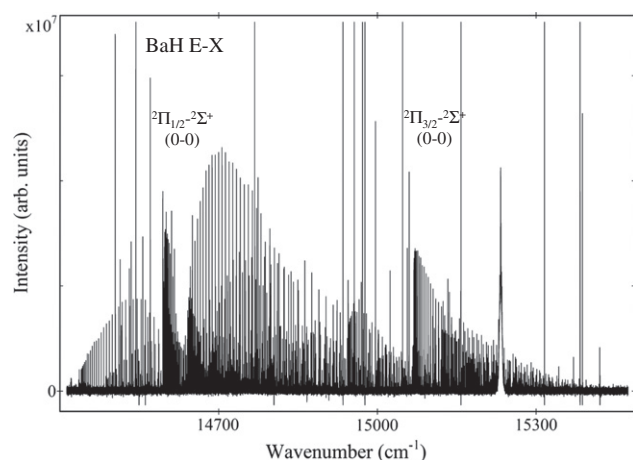


**Fig. 1.** A compressed view of the  $\Delta v = 0$  sequence, marking the two subbands of the  $E^2\Pi\text{--}X^2\Sigma^+$  transition of BaH.

The  $E^2\Pi$  state of BaH belongs to Hund's case (a) coupling and each band of the  $E^2\Pi\text{--}X^2\Sigma^+$  transition is expected to consist of six main ( $P_1, Q_1, R_1, P_2, Q_2, R_2$ ) and six satellite ( $R_{12}, Q_{12}, P_{12}, R_{21}, Q_{21}, P_{21}, R_{21}$ ) branches. All of these branches have been identified in the measured bands, although the satellite branches in the 2–2 bands appear with very weak intensity. The two sub-bands of BaH are widely separated because of large spin–orbit splitting of  $A_0 \approx 462\text{ cm}^{-1}$  in the  $E^2\Pi$  state. This observation is in contrast with the observation of this same transition in CaH where  $A_0 = 24\text{ cm}^{-1}$ . The two subbands of CaH are close and consist of only the main branches since the  $E^2\Pi$  state of CaH is nearer to Hund's case (b) coupling [28]. The  $E^2\Pi$  state of SrH with  $A_0 = 111\text{ cm}^{-1}$  [29] also has Hund's case (a) coupling.

An expanded portion of the spectrum of the 0–0 band is presented in Fig. 2 in which some rotational lines of the head-forming  $P_{11}$  and  $Q_{12}$  branches have been marked. We have identified rotational lines up to  $J = 50.5, 29.5$  and  $31.5$  in the strongest branches of the 0–0, 1–1 and 2–2 bands. We have observed several perturbations in the three observed vibrational levels of the  $^2\Pi$  state. For the  $v = 0$  vibrational level of the  $^2\Pi_{1/2}$  state, both  $e$ - and  $f$ -parity levels are perturbed near  $J = 26.5$ . The  $f$ -parity levels are also affected at higher  $J$  values and lines with  $J > 29.5$  have to be de-weighted because of perturbations at higher  $J$  values. For the  $^2\Pi_{3/2}$  component, the  $e$ -levels are perturbed near  $J = 20.5$  and  $35.5$ , while the  $f$ -levels are perturbed near  $J = 10.5, 19.5$  and  $42.5$ . Also the lines with  $J > 44.5$  have to be de-weighted due the effects of perturbations at the higher  $J$  values. For the  $v = 1$  vibrational level, perturbations were observed at  $J = 13.5$  and  $14.5$  for the  $e$ - and  $f$ -levels, respectively, of the  $^2\Pi_{1/2}$  component. For the  $v = 2$  vibrational level of the  $^2\Pi_{1/2}$  component, the lower  $J$  rotational lines are affected by strong perturbations and lines below  $J < 9.5$  of the  $e$ -parity level and  $J < 19.5$  were de-weighted. Also small local perturbations were observed near  $J = 20.5$  of the  $e$ - and  $J = 25.5$  of the  $f$ -parity levels. The  $^2\Pi_{3/2}$  component of this vibrational level is affected by perturbations near  $J = 9.5$  and  $7.5$  of the  $e$ - and  $f$ -parities, respectively. The lines affected by perturbations were given lower weights or were de-weighted completely.

In order to determine the rotational constants, the observed rotational line positions of different bands were fitted with the effective  $N^2$  Hamiltonian of Brown et al. [30]. The  $^2\Pi$  and  $^2\Sigma^+$  matrix elements of this Hamiltonian are provided by Douay et al. [31] and Amiot et al. [32]. The lines in each vibrational band were initially fitted separately using a nonlinear least-squares procedure. The infrared vibration–rotation measurements available from the previous studies [25,26] were also included with our measure-

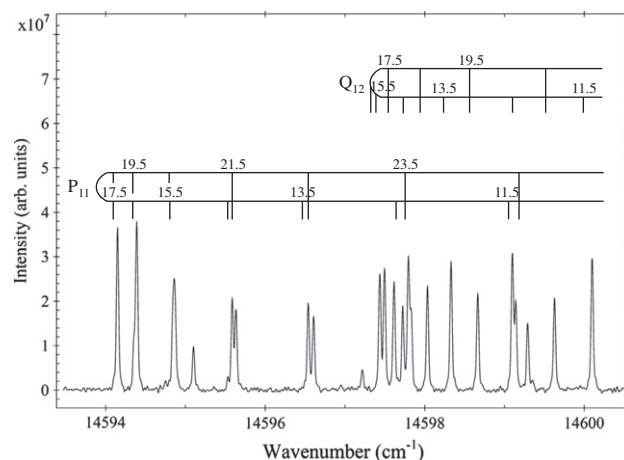


**Fig. 2.** An expanded portion of the 0–0 band near the  $P_{11}$  and  $Q_{12}$  heads. Some rotational lines of the two branches are marked.

**Table 1**  
Spectroscopic constants (in  $\text{cm}^{-1}$ ) of the  $X^2\Sigma^+$  and  $A^2\Pi$  electronic states of BaH.

State	Constants	$\nu = 0$	$\nu = 1$	$\nu = 2$	$\nu = 3$
$X^2\Sigma^+$	$T_v$	0.0	1139.289606(95)	2249.60618(14)	3331.11924(19)
	$B_v$	3.3495907(28)	3.2838078(27)	3.2179014(30)	3.1518703(34)
	$D_v \times 10^4$	1.127057(64)	1.124169(66)	1.120664(86)	1.117085(92)
	$H_v \times 10^9$	2.9837(39)	3.0061(45)	2.9994(76)	2.9859(74)
	$\gamma_v$	0.192063(30)	0.187039(30)	0.182065(33)	0.177109(37)
	$\gamma_{Dv} \times 10^5$	-1.3316(33)	-1.3226(35)	-1.3220(50)	-1.2984(50)
	$A_v$	14856.63369(38)	16047.20902(65)	17206.448(12)	-
$A^2\Pi$	$A_v$	461.85585(79)	469.9424(13)	472.883(22)	-
	$A_{Dv}^a \times 10^2$	2.02123(76)	2.1122(28)	2.9827(80)	-
	$A_{Hv} \times 10^6$	-1.1344(88)	1.558(99)	-3.29(17)	-
	$B_v$	3.4868233(40)	3.414457(14)	3.335697(75)	-
	$D_v \times 10^4$	1.167801(85)	1.19689(98)	1.0930(24)	-
	$H_v \times 10^9$	2.8399(50)	3.087(41)	-1.803(97)	-
	$q_v \times 10^2$	0.3475(19)	0.3365(27)	1.604(73)	-
	$q_{Dv} \times 10^5$	-0.1552(36)	-0.1276(53)	-7.00(34)	-
	$q_{Hv} \times 10^8$	0.0369(17)	-	5.74(17)	-
	$p_v$	0.872460(93)	0.88520(24)	1.3956(36)	-
	$p_{Dv} \times 10^3$	-0.18222(50)	-0.1470(31)	-1.481(12)	-
	$p_{Hv} \times 10^7$	0.1273(49)	-	8.02(21)	-

Note: Numbers in parentheses are one standard deviation in the last digits quoted.

<sup>a</sup> A constant  $\gamma_{H0} = -3.909(92) \times 10^{-8} \text{ cm}^{-1}$  was also determined for  $\nu = 0$ .

ments using suitable weights based on the uncertainties provided in the original papers. The weights for the weaker and blended lines were chosen according to the signal-to-noise ratio and extent of blending. The spectroscopic parameters  $T_v$ ,  $A_v$ ,  $A_{Dv}$ ,  $A_{Hv}$ ,  $B_v$ ,  $D_v$ ,  $H_v$ ,  $q_v$ ,  $q_{Dv}$ ,  $q_{Hv}$ ,  $p_v$ ,  $p_{Dv}$  and  $p_{Hv}$  were determined for the  $E^2\Pi$  state. A constant  $\gamma_{Hv}$  was also required for the  $\nu = 0$  vibrational level. For the ground state, the constants  $T_v$  (except  $\nu = 0$ ),  $B_v$ ,  $D_v$ ,  $H_v$ ,  $\gamma_v$  and  $\gamma_{Dv}$  were determined. Several higher order spectroscopic constants such as  $q_{Dv}$ ,  $q_{Hv}$ ,  $p_{Dv}$ , and  $p_{Hv}$  of the upper state, required to minimize the standard deviation of the fit, are a reflection of presence of interactions in the excited state. The precision of our Fourier transform measurements is greater than those of Frederickson and Watson [1] and Funke [2]; therefore considerable improvement is expected in the present spectroscopic constants.

A list of measured rotational lines of BaH bands used in the determination of the final spectroscopic constants, along with their obs.-calc. residuals is available as Supplement 1 on ScienceDirect (www.sciencedirect.com) and as part of the Ohio State University Molecular Spectroscopy Archives (http://msa.lib.ohio-state.edu/jmsa\_hp.htm). The term values for the observed vibrational levels of the  $E^2\Pi$  and  $X^2\Sigma^+$  states were calculated using the spectroscopic constants obtained in the final fit. A list of calculated term values is provided in Supplement 2. Since the ground state molecular parameters are known with excellent precision from the previous infrared studies [25,26], the present study was intended to improve the molecular constants for the excited  $E^2\Pi$  state. It is therefore interesting to compare the present excited state constants for the  $E^2\Pi$  state of BaH with the values obtained previously by Frederickson and Watson [1] and Funke [2]. For the  $\nu = 0$  vibrational level of the  $E^2\Pi$  state, our analysis provides  $T_0 = 14856.63369(38) \text{ cm}^{-1}$ ,  $A_0 = 461.85585(79) \text{ cm}^{-1}$ ,  $B_0 = 3.4868233(40) \text{ cm}^{-1}$  and  $D_0 = 1.167802(85) \times 10^{-4} \text{ cm}^{-1}$ . Frederickson and Watson [1] did not report the band origin but estimate a value of  $A_0 \approx 462 \text{ cm}^{-1}$  which is in good agreement with our value. Also, they did not report the case (a) rotational and distortion constants since they treated the  $^2\Pi_{1/2}$  and  $^2\Pi_{3/2}$  components separately, but the values of  $B_0 = 3.4812 \text{ cm}^{-1}$  and  $D_0 = 1.165 \times 10^{-4} \text{ cm}^{-1}$  were obtained from the average of the values of the two components which are also in reasonable agreement with our values. Funke [2] also determined the constants of the two components separately. Their averaged values of  $B_0 = 3.4859 \text{ cm}^{-1}$  and  $D_0 = 1.16 \times 10^{-4} \text{ cm}^{-1}$  agree well with our experimental values of

$B_0 = 3.4868233(40) \text{ cm}^{-1}$  and  $D_0 = 1.167801(85) \times 10^{-4} \text{ cm}^{-1}$ , respectively. The spectroscopic constants of the two electronic states obtained from the present analysis are provided in Table 1. The molecular constants of the different vibrational levels of the two states have been used to determine the equilibrium constants which are provided in Table 2. The ground and excited state equilibrium rotational constants  $B_e' = 3.38243550(57) \text{ cm}^{-1}$  and  $B_e'' = 3.520609(41) \text{ cm}^{-1}$  provide the equilibrium bond lengths of  $r_e'' = 2.23188651(19) \text{ \AA}$ .  $r_e' = 2.187651(13) \text{ \AA}$  for the  $X^2\Sigma^+$  and  $E^2\Pi$  states, respectively.

In a recent theoretical study Allouche et al. [22] have calculated the spectroscopic properties of all BaH states dissociating to the Ba ( $6s^2, 6s^1 5d^1, 6s^1 6p^1$ ) + H ( $^2S$ ) atomic limits. They have performed calculations with and without spin-orbit coupling and have found good agreement with the available experimental results. For example their calculated  $T_{00}$  values of the four low-lying excited states,  $A^2\Pi$ ,  $B^2\Sigma^+$ ,  $H^2\Delta$  and  $E^2\Pi$  were 9872, 11 185, 9421 and  $14967 \text{ cm}^{-1}$  compared to the experimental values of 9727.2, 10992.3, 9242.8 and  $14830.7 \text{ cm}^{-1}$ , respectively.

As in the case of other alkaline earth hydrides, most of the low-lying excited electronic states of BaH are affected by interactions with the close-lying electronic states. For example, the  $A^2\Pi$  and  $B^2\Sigma^+$  and  $H^2\Delta$  states lie very close in energy and interact strongly. The other known higher-lying electronic states are also affected by interactions. This analysis also indicates that the  $\nu = 0, 1$  and 2 vibrational levels of the  $E^2\Pi$  state are affected by perturbations. A definite assignment of the perturbing state (or states) is only possible after the characterization of other electronic states located in the same energy range. The available experimental results on

**Table 2**  
Equilibrium constants (in  $\text{cm}^{-1}$ ) of the  $X^2\Sigma^+$  and  $E^2\Pi$  states of BaH.

Constants	$X^2\Sigma^+$	$E^2\Pi$
$T_e$	0.0	14830.1578(62)
$\omega_e$	1168.42509(60)	1221.912(12)
$\omega_e x_e$	14.61366(28)	15.6682(60)
$\omega_e y_e$	0.028253(58)	-
$B_e$	3.38243550(57)	3.520609(41)
$\alpha_e$	0.06565865(69)	0.065973(79)
$\gamma_e \times 10^3$	-0.06203(17)	-3.197(39)
$r_e$ (Å)	2.23188651(19)	2.187651(13)

Note: Numbers in parentheses are one standard deviation in the last digits quoted.

BaH suggest that the  $D^2\Sigma^+$  [5] state is about  $6000\text{ cm}^{-1}$  higher in energy than the  $E^2\Pi$  state and, therefore, the perturbations to the lower vibrational levels of the  $E^2\Pi$  state are likely caused by interaction with higher vibrational levels of the  $B^2\Sigma^+$  state.

#### 4. Conclusion

The emission spectra of the  $E^2\Pi-X^2\Sigma^+$  electronic transition of BaH have been observed at high resolution using a Fourier transform spectrometer. The rotational structure of the 0–0, 1–1 and 2–2 bands has been measured and improved spectroscopic constants obtained. The equilibrium bond lengths of the  $X^2\Sigma^+$  and  $E^2\Pi$  states of BaH derived from the present analysis are  $r_e'' = 2.23188655(19)\text{ \AA}$ .  $r_e' = 2.187651(13)\text{ \AA}$ , respectively. The observed perturbations in the  $E^2\Pi$  state are likely caused by interaction with higher vibrational levels of the  $B^2\Sigma^+$  state.

#### Acknowledgments

The research described here was supported by funds from the Leverhulme Trust. The spectra used in the present work were recorded at the National Solar Observatory at Kitt Peak, USA.

#### Appendix A. Supplementary material

Supplementary data associated with this article can be found, in the online version, at <http://dx.doi.org/10.1016/j.jms.2012.12.004>.

#### References

- [1] W.R. Fredrickson, W.W. Watson, *Phys. Rev.* 39 (1932) 753–764.
- [2] G. Funke, *Z. Physik* 84 (1933) 610–628.
- [3] W.W. Watson, *Phys. Rev.* 43 (1933) 9–11; W.W. Watson, *Phys. Rev.* 47 (1935) 213–214.
- [4] P.G. Koontz, W.W. Watson, *Phys. Rev.* 48 (1935) 937–938.
- [5] I. Kopp, N. Åslund, G. Edvinsson, B. Lindgren, *Ark. Fysik.* 30 (1965) 321–357.
- [6] B. Grundstrom, *Z. Phys.* 99 (1936) 595–606.
- [7] G. Funke, B. Grundstrom, *Z. Phys.* 100 (1936) 293–306.
- [8] G. Edvinsson, I. Kopp, B. Lindgren, N. Åslund, *Ark. Fysik.* 25 (1963) 95–105.
- [9] M.A. Khan, *J. Phys. B* 1 (1968) 985–989.
- [10] M.A. Baig, M. Rafi, M.A. Khan, *Nuovo Cimento B* 40 (1977) 365–370.
- [11] M. Rafi, S. Ahmed, M.A. Khan, M.A. Baig, *Z. Phys. A* 320 (1985) 369–373.
- [12] M. Rafi, A. Al-Ghamdi, K. Ahmed, I.A. Khan, *Phys. Lett. A* 189 (1994) 304–306.
- [13] I. Kopp, M. Kronekvist, A. Guntzsch, *Ark. Fysik.* 32 (1966) 371–405.
- [14] O. Appelblad, L.E. Berg, L. Klynning, J.W.C. Johns, *Phys. Scripta* 31 (1985) 69–73.
- [15] G. Fabre, A.E. Hachimi, R. Stringat, C. Effantin, A. Bernard, J. D'Incan, J. Vergès, *J. Phys. B: At. Mol. Phys.* 20 (1987) 1933–1944.
- [16] A. Bernard, C. Effantin, J. d'Incan, G. Fabre, A. El Hachimi, R. Stringat, J. Vergès, R.F. Barrow, *Mol. Phys.* 62 (1987) 797–800.
- [17] A. Bernard, C. Effantin, J. d'Incan, G. Fabre, A.R. Stringat, R.F. Barrow, *Mol. Phys.* 67 (1989) 1–18.
- [18] R.F. Barrow, B.J. Howard, A. Bernard, C. Effantin, *Mol. Phys.* 72 (1991) 971–976.
- [19] P. Fuentealba, O. Reyes, H. Stoll, H. Preuss, *J. Chem. Phys.* 87 (1987) 5338–5345.
- [20] P. Fuentealba, O. Reyes, *Mol. Phys.* 62 (1987) 1291–1296.
- [21] M. Kaupp, P.V.R. Schleyer, H. Stoll, H. Preuss, *J. Chem. Phys.* 94 (1991) 1360–1366.
- [22] A.R. Allouche, G. Nicolas, J.C. Barthelat, F. Spiegelmann, *J. Chem. Phys.* 96 (1992) 7646–7655.
- [23] L.-E. Berg, K. Ekvall, A. Hishikawa, S. Kelly, *Phys. Scripta* 55 (1997) 269–272.
- [24] L.B. Knight Jr., W. Weltner Jr., *J. Chem. Phys.* 54 (1971) 3875–3884.
- [25] U. Magg, H. Birk, H. Jones, *Chem. Phys. Lett.* 149 (1988) 321–325.
- [26] K.A. Walker, H.G. Hedderich, P.F. Bernath, *Mol. Phys.* 78 (1993) 577–589.
- [27] W. Whaling, W.H.C. Anderson, M.T. Carle, J.W. Brault, H.A. Zarem, *J. Res. Natl. Inst. Stand. Technol.* 107 (2002) 149–169.
- [28] R.S. Ram, K. Tereszchuk, I.E. Gordon, K.A. Walker, P.F. Bernath, *J. Mol. Spectrosc.* 266 (2011) 86–91.
- [29] R.S. Ram, K. Tereszchuk, K.A. Walker, P.F. Bernath, *J. Mol. Spectrosc.* 271 (2012) 15–19.
- [30] J.M. Brown, E.A. Colbourn, J.K.G. Watson, F.D. Wayne, *J. Mol. Spectrosc.* 74 (1979) 294–318.
- [31] M. Douay, S.A. Rogers, P.F. Bernath, *Mol. Phys.* 64 (1988) 425–436.
- [32] C. Amiot, J.-P. Maillard, J. Chauville, *J. Mol. Spectrosc.* 87 (1981) 196–218.